

Study of ^{22}Ne and ^{28}Mg Excited States using Fusion-Evaporation and Doppler Shift Measurements

Jonathan Williams

PhD Candidate
Simon Fraser University
Department of Chemistry

WNPPC 2017
February 17, 2017



Gamma-ray spectroscopy and nuclear structure

- The electromagnetic force is a convenient probe of nuclear systems.
 - The electromagnetic interaction is well understood.
 - Electromagnetic interactions are much weaker than the strong interactions which bind nuclei \rightarrow a non-intrusive probe.
- Study of electromagnetic transition rates and energies via gamma-ray spectroscopy can yield information on nuclear structure.

Gamma-ray spectroscopy and nuclear structure

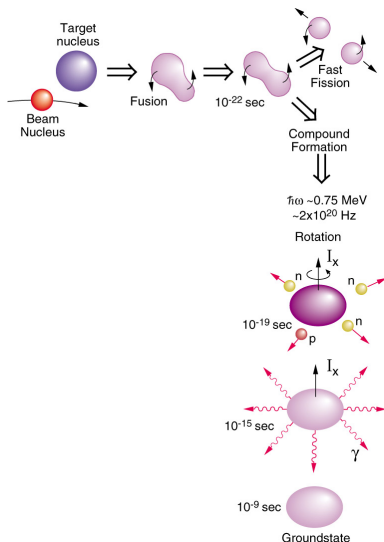
- Electromagnetic transition rates can be used to probe electric/magnetic moments of a nucleus.
- Eg. the lifetime τ of the E2 transition to a nucleus's ground state can be related to the deformation in its charge distribution β :

$$\frac{1}{\tau E_\gamma^5} \propto B(E2) \propto \beta^2$$

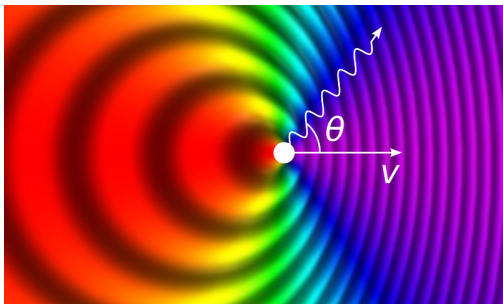
- We can measure E_γ with high precision via gamma-ray spectroscopy, τ is harder.

Fusion-evaporation reaction mechanism

- A compound system forms with large angular momentum and recoil speed.
- The system decays first by the emission of particles (forming species of interest).
- Residual nucleus (species of interest) decays by gamma-ray emission.
 - Can select specific residual nuclei via charged particle detection and identification.



Doppler shift lifetime measurements

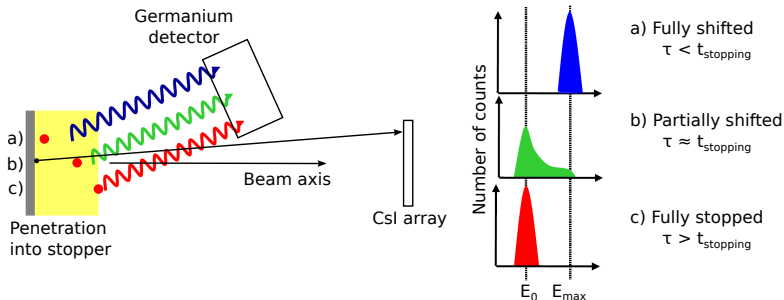


$$E_{\gamma} = E_0 \frac{\sqrt{1 - \beta^2}}{1 - \beta \cos \theta}, \quad \beta = \frac{v}{c}$$

Depending on the speed of the residual nucleus at decay time, different gamma-ray energies are detected.

- Can infer the lifetime of the state being measured from the gamma-ray energy distribution.

Doppler Shift Attenuation Method (DSAM)

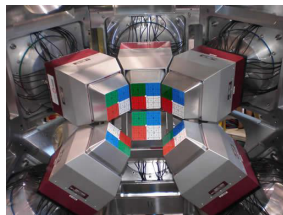


- Nucleus of interest slows and stops in a thick target backing.
- Observe lineshape depending on the speed distribution of the residual at time of gamma-ray emission.
- Nucleus stops quickly \rightarrow technique only good for $\tau < 1$ ps.

Detection Systems

Gamma ray detection: TRIUMF Gamma-Ray Escape Suppressed Spectrometer (TIGRESS)

- Array of segmented HPGe clover detectors.



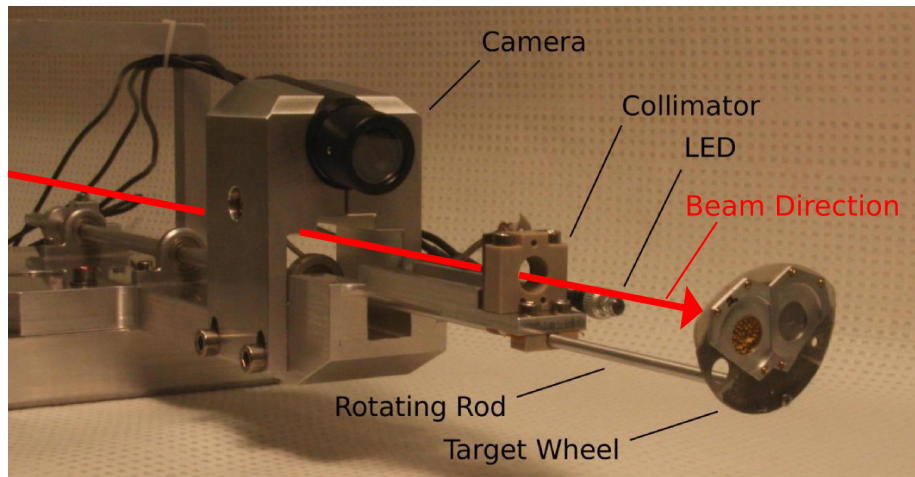
Charged particle detection: CsI(Tl) detectors

- 2 configurations: 24 element wall (pictured), ball with spherical coverage (under construction).
- Particle identification by fitting waveforms.



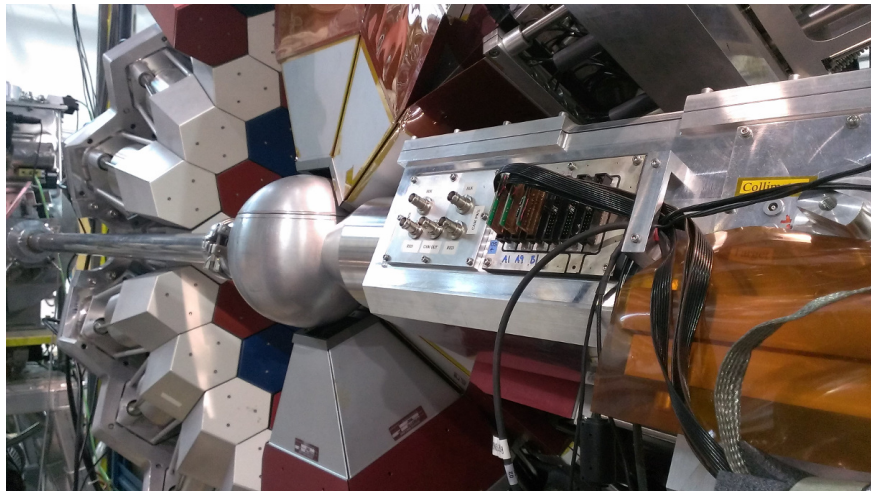
+ the **TIP** (TIGRESS Intergrated Plunger) target device.

TIP DSAM configuration



P. Voss et al. Nucl. Inst. Meth. A **746** 87 (2014)

TIP chamber in TIGRESS



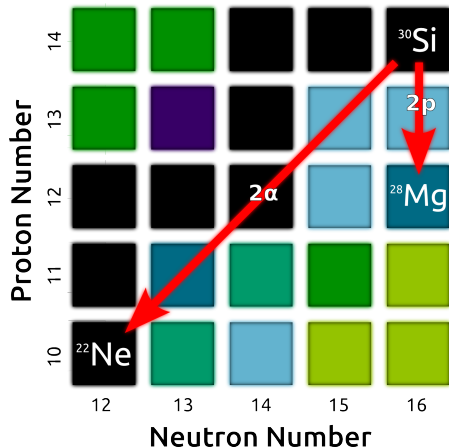
P. Voss et al. Nucl. Inst. Meth. A **746** 87 (2014)

TIP target position



P. Voss et al. Nucl. Inst. Meth. A **746** 87 (2014)

TIP/TIGRESS Commissioning experiment



TIGRESS/TIP @ TRIUMF:

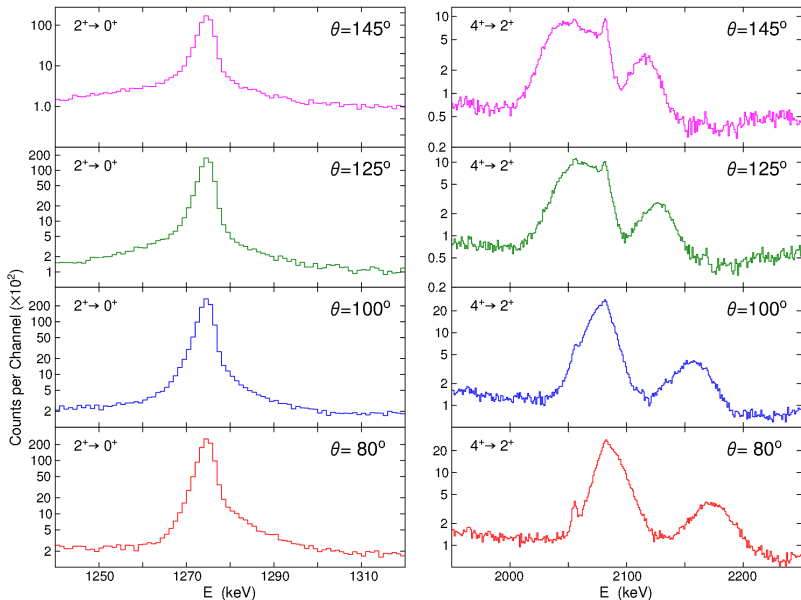
- ^{18}O beam (48 MeV)
- nat.C target (0.433 mg/cm²)
- ^{197}Au backing (28.79 mg/cm²)
- CsI(Tl) detector wall

Particles evaporate from the ^{30}Si compound nucleus to form various residual species.

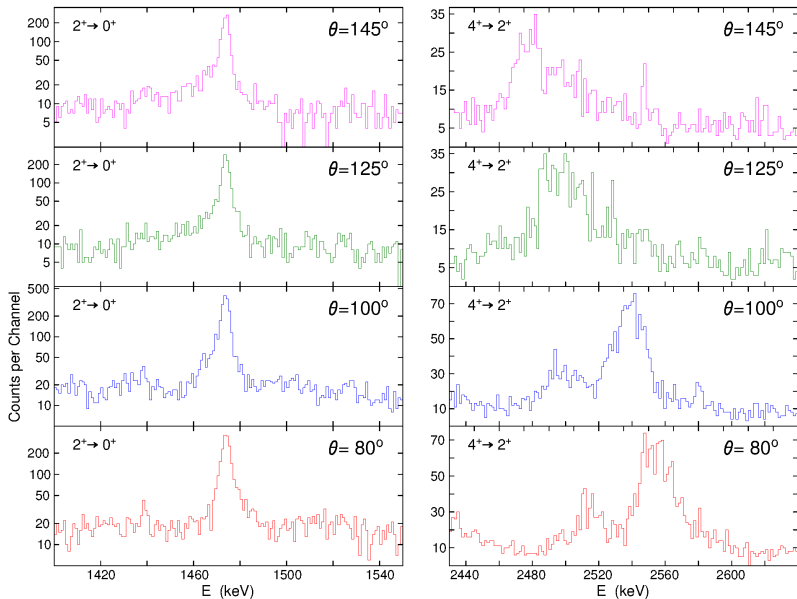
2 species of interest:

- ^{22}Ne (high statistics)
- ^{28}Mg (structure information)

^{22}Ne lineshapes



^{28}Mg lineshapes



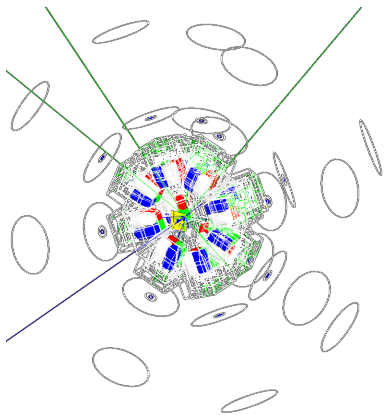
Doppler shift lineshape analysis

- Want to determine lifetimes of transitions from their lineshapes, which arise from the Doppler shift distribution of recoiling nuclei
- Many factors influence this...
 - Momentum of incoming beam
 - Momentum distribution of particles evaporated after reaction
 - Distribution of reaction positions within the target
 - Stopping of beam and reaction products inside the target/stopper
 - Geometry of the detector system(s) with respect to the reaction target
 - Other annoying things such as detection efficiencies
AND FINALLY...
 - Lifetime of the transition

Parameter space is way very large → need to simulate the process!

Doppler shift lineshape analysis code

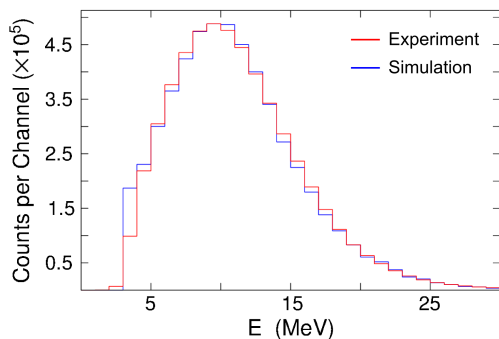
- GEANT4¹ based analysis code to extract lifetimes from DSAM lineshapes was developed, including:
 - Target, stopper, and detection system geometry
 - Fusion-evaporation reaction kinematics
- Additional code for comparing lineshapes between simulation and experiment using χ^2 analysis has been developed.



¹S. Agostinelli, et al., Nucl. Instr. Meth. Phys. Res. A 506 250303 (2003).

Fusion Evaporation in GEANT4

- Formation of compound system at a random depth in the target, followed by emission of one or more particles.
- Gamma-ray emission from the residual nucleus according to user defined lifetime.
 - GEANT4 handles particle momenta and Doppler shift of gamma rays.
 - Sequential gamma ray emission is possible (cascades).



- Evaporated particle energy distribution modelled to match experiment (Gaussian with exponential tail).

Extra details

Things we have to take into account to get the full picture:

Sequential transitions

- Transitions may be fed from higher lying states with their own lifetimes
→ affects gamma-ray lineshape
- Need to determine amount of feeding, lifetimes of higher lying states.

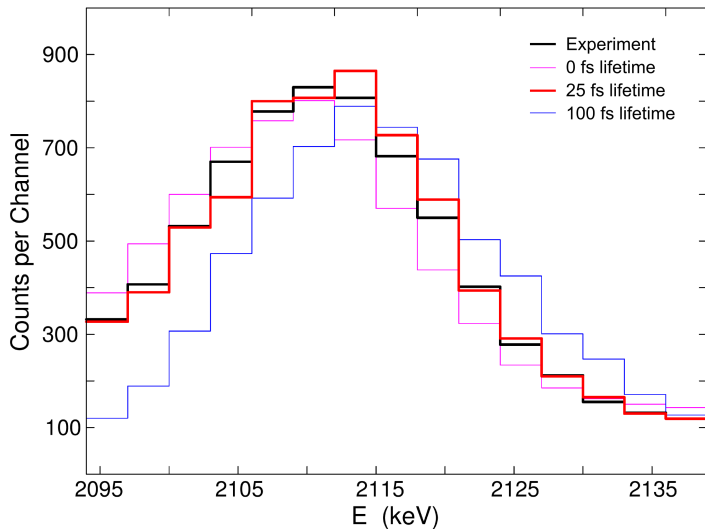
Overlapping peaks

- Need to simulate and fit all transitions simultaneously.

Response of the detector

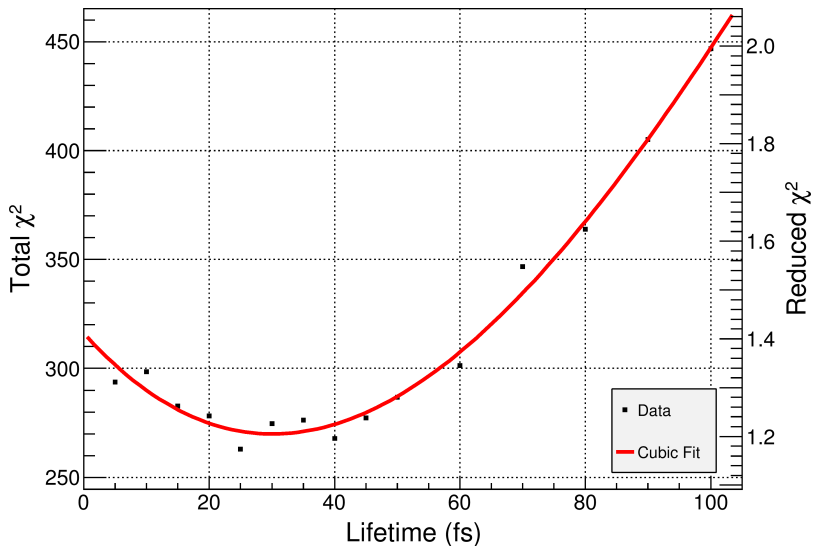
- Measured stopped peaks have non-zero width.
- Need to apply some parametrized response function to simulated data.

Lineshape vs. lifetime



Peak shape vs. simulated lifetime for the 5523 keV level in ^{22}Ne .

χ^2 statistic



χ^2 statistic vs. simulated lifetime for the 5523 keV level in ^{22}Ne .

Lifetimes in ^{22}Ne

Measured lifetimes for select observed ^{22}Ne transitions.

Evaluated E_{level} (keV) ¹	$J\pi$ ¹	Evaluated τ (fs) ¹	Measured τ (fs)
3357.2	4+	324(6)	290(50)
5146.0	2-	1200(300)	1100(200)
5523.3	(4)+	30(4)	30(10)
6311.0	(6+)	71(6)	70(5)
6345.1	4+	19(4)	11(6)
7423.0	(5+)	< 4	5(11)
8976	-	-	< 6

¹M. S. Basunia, Nuclear Data Sheets 127 (2015) 69–190.

Analysis summary

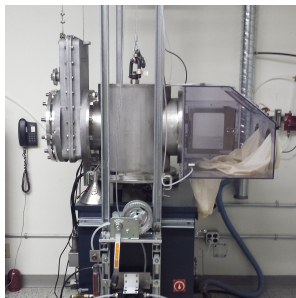
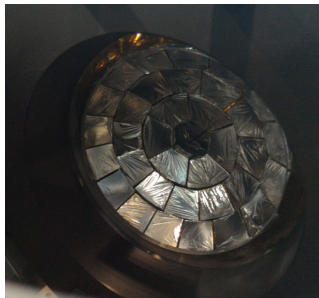
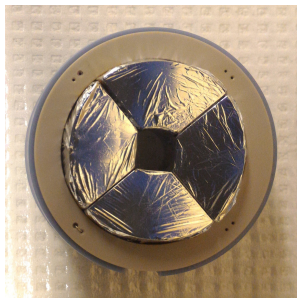
Analysis of ^{22}Ne from the commissioning run data is complete.

Have submitted a paper on the analysis procedure to Nuclear Instruments and Methods A.

- Currently under review.

Further developments

Construction of detectors and targets has begun for future experiments.



Left: CsI ball ring 0.

Centre: CsI ball used in December 2016 test run.

Right: Evaporator for target production.

Future Work

We plan to run a ^{68}Se experiment in summer/fall 2017 using $^{40}\text{Ca}(^{36}\text{Ar}, 2\alpha)^{68}\text{Se}$.

- Nuclear structure studies along the $N = Z$ line.

Possible future work:

- Analysis of ^{28}Mg data.
- Use of calcium target to study other nuclei, such as ^{56}Ni ($N = Z = 28$) via $^{40}\text{Ca}(^{21}\text{Na}, \alpha p)^{56}\text{Ni}$.

Acknowledgements

Simon Fraser University

Current: A. Chester, T. Domingo, K. Starosta

Former: R. Ashley, U. Rizwan, P. Voss

SFU Science Machine & Electronics Shops

R. Holland, P. Kowalski, J. Shoults, K. Van Wieren

TRIUMF

P. Bender, A. B. Garnsworthy, G. Hackman, R. Henderson, R. Krücken,
D. Miller, M. Moukaddam, M. Rajabali, C. Unsworth, Z.-M. Wang

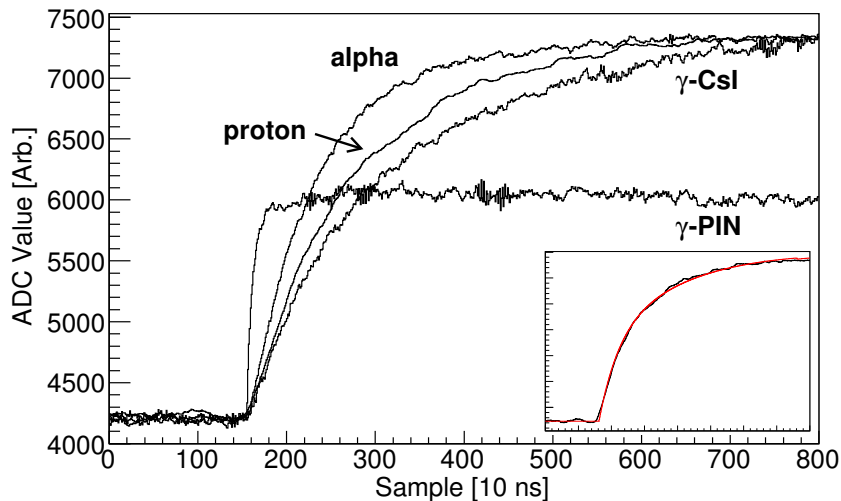
University of Guelph

B. Hadina, C. Svensson

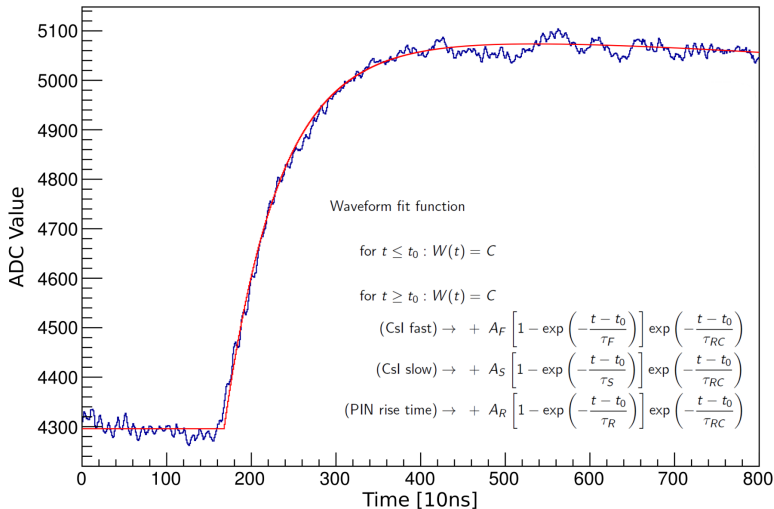


Analysis code used in this project is available at github.com/SFUNUSC

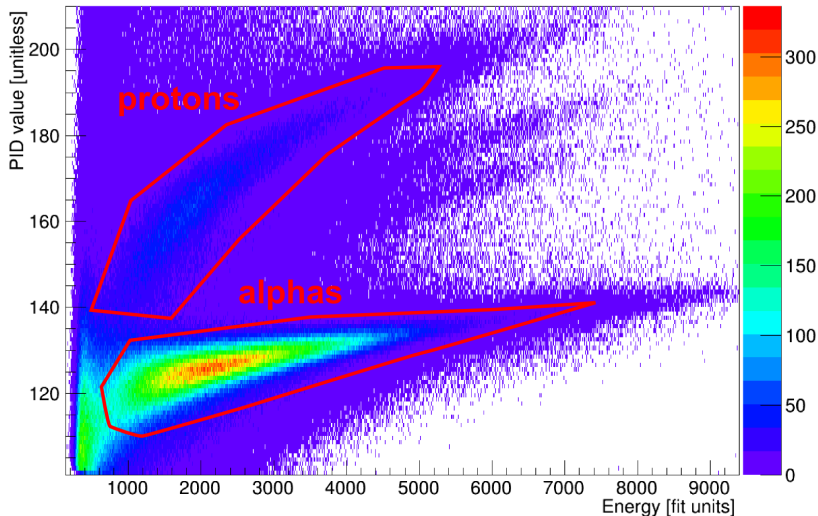
Particle identification using CsI waveform fits



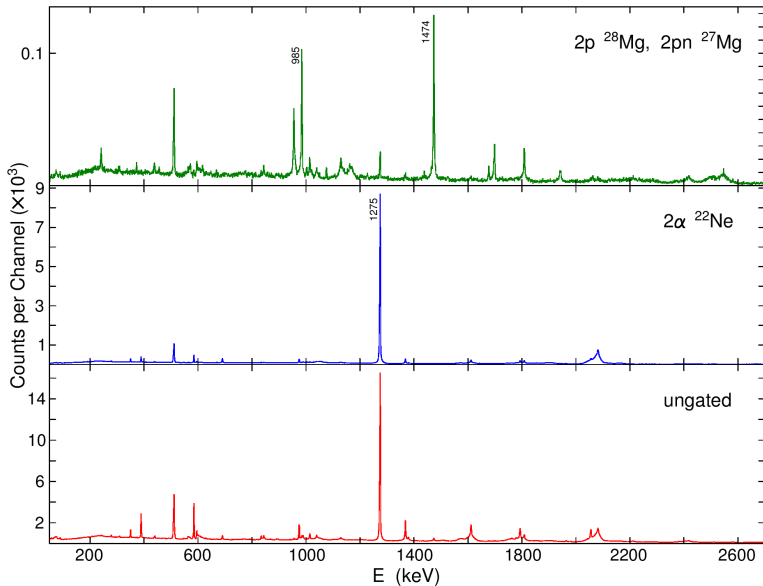
Particle identification using Csl waveform fits



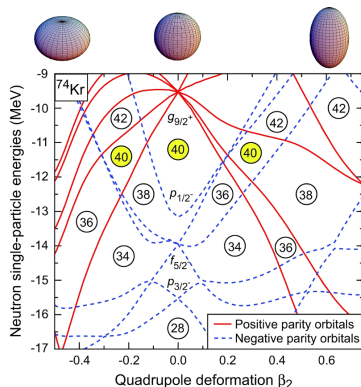
Particle identification using CsI waveform fits



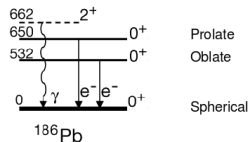
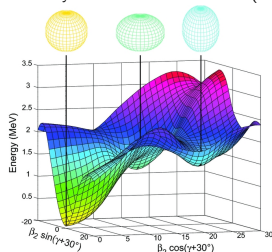
CsI(Tl) 2p and 2 α gates



Shape coexistence along the $N = Z$ line



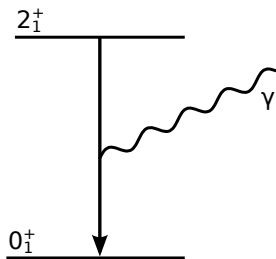
A. N. Andreyev et al. Nature **405** 430 (2000).



- Nearly degenerate shell gaps exist for positive and negative quadrupole deformations leading to shape coexistence.

Studying nuclear structure using the electromagnetic force

- The electromagnetic force provides a convenient non-intrusive probe of nuclear systems bound by the strong force.
- Lifetime measurements using gamma-ray spectroscopy provide:
 - 1 An observable sensitive to nuclear structure.
 - 2 A sensitive benchmark for nuclear model calculations.



$$\begin{aligned}\tau(E2; 2_1^+ \rightarrow 0_1^+) &= \lambda(E2; 2_1^+ \rightarrow 0_1^+)^{-1} \\ \lambda(E2; 2_1^+ \rightarrow 0_1^+) &\propto E(2_1^+)^5 \times B(E2; 2_1^+ \rightarrow 0_1^+) \\ B(E2; 2_1^+ \rightarrow 0_1^+) &= \frac{1}{5} |\langle 2_1^+ || E2 || 0_1^+ \rangle|^2 \propto \beta^2\end{aligned}$$

Recent studies in $N = Z = 34$ ^{68}Se

Model	Model calculations				
	Shell Model	Interacting Boson Model	Hartree- Bogoliubov	Self-consistent Collective Coordinate	Excited Vampir
$B(E2, 2_1^+ \rightarrow 0_1^+) [e^2\text{fm}^4]$	100 ¹	280 ²	500 ³	725 ⁴ 834 ⁴	1048 ⁵

¹M. Hasegawa et al. Phys. Lett. B **656** 51 (2007).; ²F. Il. Khudair, Y. S. Li, G. L. Long, Phys. Rev. C **75** 054316 (2007).

³T. A. War et al. Eur. Phys. J. A **22** 13 (2004).; ⁴N. Hinohara et al. Prog. Theor. Phys. (Kyoto) **119** 59 (2008).

⁵A. Petrovici et al. Nucl. Phys. A **710** 246 (2002).

Recent measurements		
Method	$B(E2, 2_1^+ \rightarrow 0_1^+) [e^2\text{fm}^4]$	τ [ps]
Coulomb Excitation ⁶	430(60)	4.2(6)
Recoil Distance Method ⁷	390(70)	4.6(8)

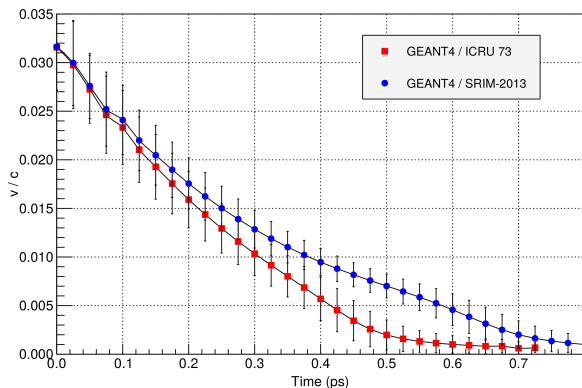
⁶A. Obertelli et al. Phys. Rev. C **80** 031304(R) (2009).

⁷A. J. Nichols et al. Phys. Rev. B **733** 52 (2014)

Stopping power comparison

Comparison of simulations using stopping powers from ICRU73¹ (GEANT4 default) and SRIM² was performed.

For transitions with short lifetimes (< 0.2 ps) the effect on the source speed distribution is $\leq 10\%$.

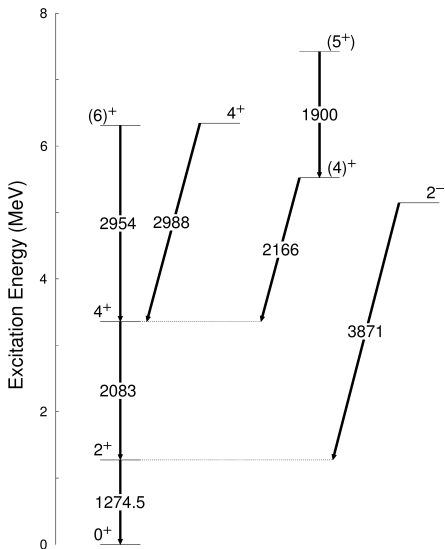


Residual nucleus speed in gold as a function of stopping time. Initial residual energy distribution taken from full simulations.

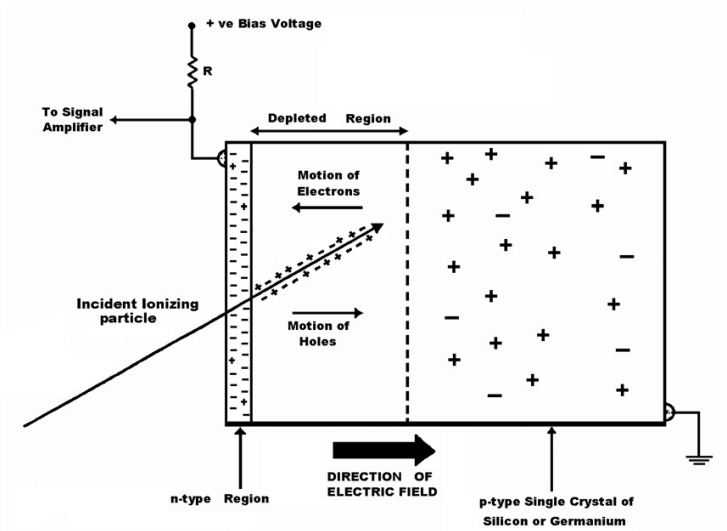
¹ICRU Report 73, J. ICRU **5(1)** 1 (2005)

²J. Ziegler et al., Nucl. Instr. Meth. Phys. Res. B **268** 1818 (2010)

^{22}Ne level scheme



Semiconductor detector (eg. HPGe) schematic



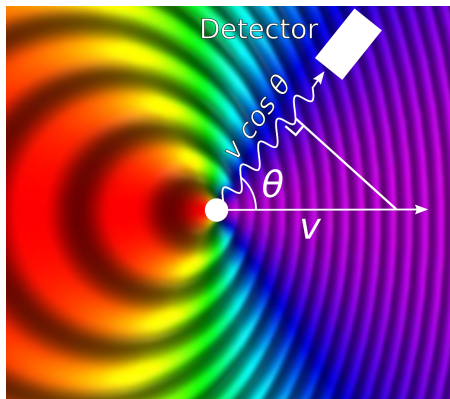
Relativistic Doppler effect

For photons:

$$E = hf \text{ (energy)}$$

$$\lambda = c/f \text{ (wavelength)}$$

$$T = 1/f \text{ (wave period)}$$



Other definitions:

$$\beta = v/c$$

$$\gamma = \frac{1}{\sqrt{1-\beta^2}}$$

From non-relativistic Doppler shift:

$$\begin{aligned} \lambda_{obs} &= \frac{c}{f_{obs}} = \frac{c - v_{||}}{f_{src}} \\ &= \frac{c - v_{src} \cos \theta}{f_{src}} \end{aligned}$$

$$\begin{aligned} \frac{f_{obs}}{f_{src}} &= \frac{T_{src}}{T_{obs}} = \frac{c}{c - v_{src} \cos \theta} \\ &= \frac{1}{1 - \beta \cos \theta} \end{aligned}$$

Relativistic Doppler effect (cont.)

From time dilation (special relativity):

$$T_{src} = \frac{T_{obs}}{\gamma}, \gamma = \frac{1}{\sqrt{1 - \beta^2}}$$

$$\frac{f_{obs}}{f_{src}} = \frac{T_{src}}{T_{obs}} = \frac{1}{\gamma} = \sqrt{1 - \beta^2}$$

Combining Doppler shift and time dilation:

$$\frac{f_{obs}}{f_{src}} = \frac{\sqrt{1 - \beta^2}}{1 - \beta \cos \theta}$$

$$E_{obs} = E_{src} \frac{\sqrt{1 - \beta^2}}{1 - \beta \cos \theta}$$

Semi-empirical mass model¹

Model treating the nucleus like a liquid drop, with shell model correction terms:

$$BE(A, Z) = a_V A - a_S A^{2/3} - a_C \frac{Z(Z-1)}{A^{1/3}} - a_A \frac{(A-2Z)^2}{A} + \Delta E_{pair}$$

Deformation from sphericity affects the surface and Coulomb terms, eg. for ellipsoidal deformation:

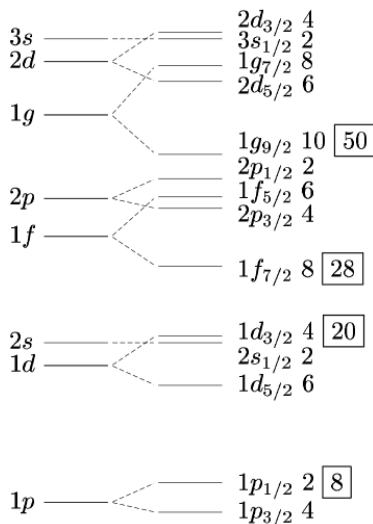
$$\begin{aligned} a_S A^{2/3} &\rightarrow a_S A^{2/3} (1 + (2/5)\epsilon^2) \\ a_C \frac{Z(Z-1)}{A^{1/3}} &\rightarrow a_C \frac{Z(Z-1)}{A^{1/3}} (1 - (1/5)\epsilon^2) \\ \epsilon &= \sqrt{1 - b^2/a^2} \quad (\text{minor/major axis length ratio}) \end{aligned}$$

¹K. Heyde, Basic Ideas and Concepts in Nuclear Physics, IOP Publishing, 2004.

Nuclear shell model

Similar to electron shell model. Main differences:

- Flat-bottom potential representing nuclear interaction.
- Protons and neutrons have their own shells.
- Strong spin-orbit coupling results in different magic numbers.
 - Due to spin dependence of the nuclear interaction, from coupling of a nucleon's spin and its orbital angular momentum (which depends on the mean field produced by all nucleons).



Fermi's golden rule

Transition rate depends on initial and final wavefunctions, interaction V_p which causes the transition, and density of final states $\rho(E_f)$.

$$\lambda = \frac{2\pi}{\hbar} \left| \int \psi_f^* V_p \psi_i dv \right|^2 \rho(E_f)$$
$$\propto |\langle \psi_f | V_p | \psi_i \rangle|^2$$

So for an E2 transition:

$$\lambda \propto \frac{1}{5} |\langle 2_1^+ || E2 || 0_1^+ \rangle|^2 = B(E2; 2_1^+ \rightarrow 0_1^+)$$

Weisskopf estimates¹

Estimates of reduced transition probabilities assuming a single particle transition and nucleus with uniform density, radius $R = r_0 A^{1/3}$.

$$B(EL) = \frac{1}{4\pi} \left[\frac{3}{L+3} \right]^2 (r_0)^{2L} A^{2L/3} [e^2 fm^{2L}]$$
$$B(ML) = \frac{10}{\pi} \left[\frac{3}{L+3} \right]^2 (r_0)^{(2L-2)/2} \mu_n^2 [e^2 fm^{2L-2}]$$

μ_n - magnetic moment of particle of interest.

¹W. Loveland, D. J. Morrissey, G. T. Seaborg, Modern Nuclear Chemistry, Wiley, 2006.

Nuclear charge distribution¹

Potential arising from charge distribution $\rho(\vec{r})$ of nucleons at a distance \vec{R} :

$$\Phi(\vec{R}) = \frac{1}{4\pi\epsilon_0} \int_{Vol} \frac{\rho(\vec{r})}{|\vec{R} - \vec{r}|} d\vec{r}$$

Expanded in $|\vec{r}/\vec{R}|$:

$$\Phi(\vec{R}) = \frac{1}{4\pi\epsilon_0} q/R + \sum_i \frac{p_i}{4\pi\epsilon_0} \frac{X_i}{R^3} + \sum_{ij} \frac{1}{2} \frac{1}{4\pi\epsilon_0} \frac{Q_{ij}}{R^5} X_i X_j + \dots$$

$$p_i = \int \rho(\vec{r}) x_i d\vec{r},$$
$$Q_{ij} = \int \rho(\vec{r}) (3x_i x_j - r^2 \delta_{ij}) d\vec{r}.$$

with $i = 1, 2, 3$ corresponding to Cartesian coordinates x, y, z .

¹K. Heyde, Basic Ideas and Concepts in Nuclear Physics, IOP Publishing, 2004.